Effect of the precursor and reduction methods on the synthesis of supported Pt nanostructures in zeolite mordenite

Leonel Quiñones · María M. Martínez-Iñesta

Abstract In this article, the effect of the metal precursor and of the reduction methods in the formation of anisotropic nanostructures using zeolite mordenite as template is explored. Reducing agents in the gas, liquid, and solid phase were studied in some cases at various temperatures. In general, $HPtCl_6$ has a tendency to form anisotropic Pt structures but on the surface of the zeolite regardless of the reduction method, while $Pt(NH_3)_4(NO_3)_2$ lead to diverse Pt nanostructures inside the pores of the zeolite. It was evident that the anisotropy of the platinum nanostructures formed increased following the sequence of Gas < Liquid < Solid. Overall, the formation of Pt nanostructures that include dispersed nanoclusters, nanoparticles, multipods, nanoflowers, and nanowires obtained with the different reduction methods is discussed.

Introduction

Platinum nanostructures are very attractive due to the physical and chemical properties they exhibit as a function of size, shape, and crystalline configuration [1]. They are being widely studied for integration into devices such as fuel cells and biosensors [1, 2].

As an example, platinum nanocluster-modified electrodes have shown good sensitivity and stability for the detection of glucose, hydrogen peroxide, and DNA [3–6]. Meanwhile, platinum nanowires arranged in a nanoelectrode assembly have been shown to provide sensitivity for the detection of peroxide that is 50 times higher, when compared with conventional platinum disk electrodes [7].

Platinum nanowires are some of the most interesting and promising nanostructures because, due to their morphology, they can exhibit quantum confinement effects of electrons axially [1]. Further development of Pt nanowires could potentially enable novel applications in fields such as catalysis, gas absorption, and electron transport [2, 8].

The template method has proven to be an efficient bottom-up approach to synthesizing small platinum nanostructures [9–14]. There are two main synthetic routes to generate templated platinum nanostructures: using hard templates and soft templates. The hard template route is focused on the reduction of the metal inside a solid porous matrix, while the soft template is associated with the reduction of the metal in the presence of a capping surfactant or organic solvent.

Solid porous templates can be classified according to their pore size in microporous, mesoporous, and macroporous materials [1, 11]. Macroporous materials are those with pore sizes above 50 nm, such as porous alumina. Materials with a pore size of 2–50 nm are classified as mesoporous, the most common of which is mesoporous silica, and microporous materials have pores with a diameter less than 2 nm, as in the case of zeolites [15]. Once incorporated into the template, the metal precursor is reduced to form the final metallic structure.

Articles on the synthesis of Pt nanoparticles abound. In macroporous materials such as anodic aluminum oxide (AAO), platinum nanoparticles, nanotubes and nanowires have been synthesized by the reduction of the metal with, for example, sodium borohydride and by electrochemical deposition [3, 13, 16]. In mesoporous silicas, metal nanoclusters are usually synthesized by thermal reduction with hydrogen gas [12, 17–22], while metal nanowires

L. Quiñones · M. M. Martínez-Iñesta (✉)
Chemical Engineering Department, University of Puerto Rico,
Mayagüez, PR 00680, USA
e-mail: mariam.martinez@upr.edu

have been synthesized using less traditional reduction methods, such as water saturated hydrogen in hierarchically ordered mesocellular mesoporous silica (HMM) [21], photo-reduction with methanol using UV light in HMM-1 [12], and sodium borohydride in solution in mesoporous silica MCM-41 [10].

Using soft templates, Chen and co-workers [23] reported the synthesis of single crystal "sea urchin" platinum nanowires, using a polyol process at 110 °C, H_2PtCl_6 as the platinum precursor, and ethylene glycol as a reducing agent. In this study, the temperature was a critical parameter to obtain the nanostructures, as no Pt nanoparticles formed at room T. Similarly, Herrichs and coworkers [24] obtained morphological control over platinum nanostructures using H_2PtCl_6 as a precursor and ethylene glycol as a reducing agent. In this study, the reduction of the precursor was controlled with $NaNO_3$ at room temperature. When the molar ratio between $NaNO_3$ and H_2PtCl_6 was increased from 0 to 11, the morphology of the platinum nanostructures changed from spheroidal particles toward more irregular structures (tetrahedral o octahedral), presumably due to the slowing of the reduction reaction.

An alternative synthetic route that was template- and surfactant-free was developed by Sun et al. to obtain platinum nanoflowers. In this synthesis method, H_2PtCl_6 was mixed with an aqueous solution of formic acid at room temperature and at atmospheric pressures for up to 16 h. When the synthesis was done at higher temperatures (50 °C and 80 °C), the formation of nanoparticles was favored, as the reduction was much faster than at room temperature [25].

These studies show that when the rate of reduction is lowered without being suppressed, the formation of anisotropic nanostructures is preferred by becoming a Pt diffusion dominated process [14, 23–26].

In microporous materials, on the other hand, even though synthesis of platinum nanoclusters has been well studied for catalytic applications [27, 28], synthesis methods to obtain anisotropic platinum nanostructures are scarce. If microporous materials such as zeolites are successfully used as templates for the formation of anisotropic structures, it would lead to the formation of a vast range of very small nanostructures that would mimic more than 190 different zeolite pore structures.

In a previous article, our research group reported the formation of platinum nanowires with a diameter of 6.57 nm inside the pores of the zeolite mordenite using the precursor $Pt(NH_3)_4(NO_3)_2$ using $NaBH_4$ in the solid state as a reducing agent [29]. Zeolite mordenite is chosen because it has 1D pore channel structures that could promote the formation of nanowires and because it has a high concentration of tetrahedrally coordinated alumina which could promote the even dispersion of positively charged Pt precursors.

In general, this article explores how the different precursors and reduction methods discussed above affect the structure of the Pt when using zeolite mordenite as a template. The result is a wide range of nanostructures: nanoparticles, nanoflowers, multipods, and nanowires. While discussing the results, this article aims to explain why the solid-state reduction method is necessary for the formation of Pt nanowires in zeolites.

Chemicals and materials

Na-Mordenite (CBV-12A) with a Si/Al = 6.5 was purchased from the company Zeolyst International. Chloroplatinic acid hydrate ($H_2PtCl_6.H_2O$) and tetraamineplatinum (II) nitrate ($Pt(NH_3)_4(NO_3)_2$) were obtained from Alfa Aesar/Johnson Matthey. Ultra high purity gas Nitrogen (N_2, 99.9999% pure) and hydrogen (H_2, 99.9999% pure) were obtained from Linde Gas. Ethylene glycol ($HOCH_2CH_2OH$) and methanol (CH_3OH, 99.8%) were acquired from Fisher chemical (USA). Formic acid (ACS, 96+ %) and potassium borohydride (KBH_4, 98%) were obtained from Alfa Aesar company.

Experimental section

Zeolite mordenite was pretreated in vacuum (10 µmHg) at 400 °C for a period of 12 h to remove any impurities present in their pores. Pretreated 200 mg mordenite samples were then impregnated with the aqueous solution of $PtCl_6^{-2}$ and $Pt(NH_3)_4^{+2}$ via incipient wetness impregnation to achieve a platinum concentration of 5% wt and are referred to as $PtCl_6^{-2}$/MOR and $Pt(NH_3)_4^{+2}$/MOR, respectively. These impregnated samples were subsequently reduced with each of the six methods described below and their variants.

In the reduction method A, the samples were placed into a tubular reactor on a ceramic boat, where the samples were heated at a temperature ramp rate of 2.91 °C/min under H_2 gas (50 mL/min, 99.999%) from 25 to 200 °C, and maintained at 200 °C for 2 h. Then, the samples were cooled under nitrogen gas (50 mL/min, 99.9999%). The samples were heated at a temperature of 200 °C to induce the complete thermal reduction of the metal precursor. These are the conditions optimized by Fukuoka et al. in mesoporous silicas [21].

Also following the study by Fukuoka and coworkers [21], in reduction method B, the samples were placed into a tubular reactor on a ceramic boat where the samples were heated at a temperature ramp of 2.91 °C/min under hydrogen gas saturated with water vapor (H_2, 50 mL/min, 99.999%) from 25 to 200 °C, and maintained at 200 °C for

2 h. Later, the samples were cooled under nitrogen gas (50 mL/min, 99.9999%).

Reduction method C was inspired by the study of Sun et al. [25] in template-less systems, and it consisted of adding formic acid (50 µl) drop by drop onto the samples of Pt/MOR. The reactions were carried out at room temperature for 48 h, where the samples were mixed in intervals of 8 h until they achieved the gray color characteristic of reduced platinum. The same reduction method was done at 110 °C and is denoted as 'C.'

In reduction method D, ethylene glycol was used as a reducing agent. The procedure consisted of adding ethylene glycol (50 µl) drop by drop onto the samples (Pt/MOR) at room temperature. After adding ethylene glycol, the samples were placed in an isothermal furnace at a controlled temperature of 110 °C for 48 h where the samples were stirred for a short period of time every 8 h. The temperature in this case was raised to 110 °C following the study by Chen [23]. The same reduction method was also done at 200 °C and is denoted as D'.

Following the reduction method described by Sakamoto et al. [30], in reduction method E, the samples were impregnated with 50 µl of methanol and put under vacuum for 2 h. Then the samples were exposed to UV light for 48 h and were stirred at intervals of 4 h until they achieved a gray color.

In the final method F, the samples of Pt/MOR were thoroughly mixed with potassium borohydride powder (KBH$_4$) using the procedure described in a previous article by our group using a 10:1 KBH$_4$:Pt ratio [29]. The reduction methods are summarized in Table 1.

Characterization

The morphology of the platinum nanostructures was characterized by transmission electron microscopy (TEM) using a Carl Zeiss Leo 922. The sample preparation for TEM analysis consisted of suspending the sample in isopropanol and applying vibration for 1 min. A 17 µL drop of the solution was added to an ultrathin carbon grid which was dried at room temperature.

Results and discussion

Figure 1a shows that the platinum nanoparticles were formed on the surface of mordenite (MOR) when the PtCl$_6^{-2}$/MOR sample was reduced with method A. The nanoparticles have an average size of 77 nm (SD = 3 nm) and have a solid core but also have a rough surface that suggest that nanowire-like structures have formed on it. On the other hand, Fig. 1b shows that well-dispersed platinum

Table 1 Summary of experimental reduction conditions

Reduction method	Platinum precursor	Reducing agent and experimental conditions
A	Pt(NH$_3$)$_4^{+2}$ PtCl$_6^{-2}$	H$_2$ gas at 200 °C for 2 h
B	Pt(NH$_3$)$_4^{+2}$ PtCl$_6^{-2}$	Hydrogen gas saturated with water vapor at 200 °C for 2 h
C	Pt(NH$_3$)$_4^{+2}$ PtCl$_6^{-2}$	Formic acid at room temperature for 48 h
C'	Pt(NH$_3$)$_4^{+2}$ PtCl$_6^{-2}$	Formic acid at 110 °C temperature for 48 h
D	Pt(NH$_3$)$_4^{+2}$ PtCl$_6^{-2}$	Ethylene glycol at 110 °C for 48 h
D'	Pt(NH$_3$)$_4^{+2}$ PtCl$_6^{-2}$	Ethylene glycol at 200 °C for 48 h
E	Pt(NH$_3$)$_4^{+2}$ PtCl$_6^{-2}$	Methanol and put under vacuum and UV light for 48 h
F	Pt(NH$_3$)$_4^{+2}$ PtCl$_6^{-2}$	Solid potassium borohydride at room temperature for 48 h

nanoclusters are formed inside mordenite when using Pt(NH$_3$)$_4^{+2}$ and the same reduction method. The nanoclusters have an average diameter of 3.9 nm (SD = 1 nm), a typically reported size for platinum nanoclusters formed inside zeolites. [31, 32]. In this article, nanoclusters are differentiated from nanoparticles by their size; the term nanoclusters is used for nanoparticles that are less than 10 nm in diameter.

These two TEM images suggest that the negatively charged precursor had difficulty incorporating into the zeolite while the positively charged was able to incorporate easily. This is probably due to the repulsion of the negatively charged mordenite structure. The tendency for the formation of nanostructures on the surface of the zeolite when using PtCl$_6^{-2}$ as a precursor was observed with the other reduction methods studied as well. As a consequence, in general, the nanostructures formed using PtCl$_6^{-2}$ grew to form larger particles. A similar result was found by Rivallan et al. [33].

TEM images of platinum nanostructures that were formed by the reduction method B are shown in Fig. 2. Figure 2a shows that for the PtCl$_6^{-2}$/MOR sample, platinum nanoflower-like structures are formed on the surface of the zeolite. The nanostructures had an average core diameter of 81 nm (SD = 15 nm) surrounded by nanowires approximately 33 nm in length and 5 nm in diameter. When compared with the results by Fukuoka [21], who used this same precursor and reducing method here, the same tendency to form anisotropic nanostructures is observed with the difference that in mordenite they are formed on the surface of a core particle grown on the
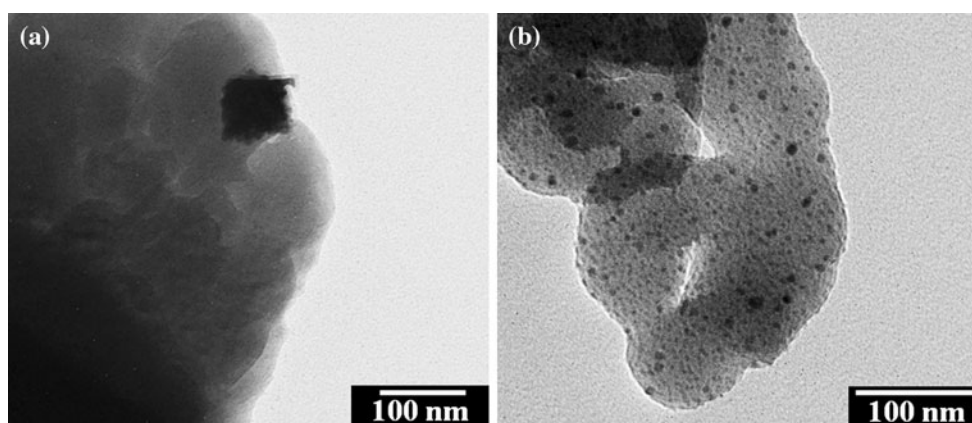
Fig. 1 Bright field TEM images of **a** platinum nanoparticles and **b** platinum nanoclusters obtained after the reduction of the $PtCl_6^{-2}$/MOR and $Pt(NH_3)_4^{+2}$/MOR samples, respectively, with H_2 (method A)
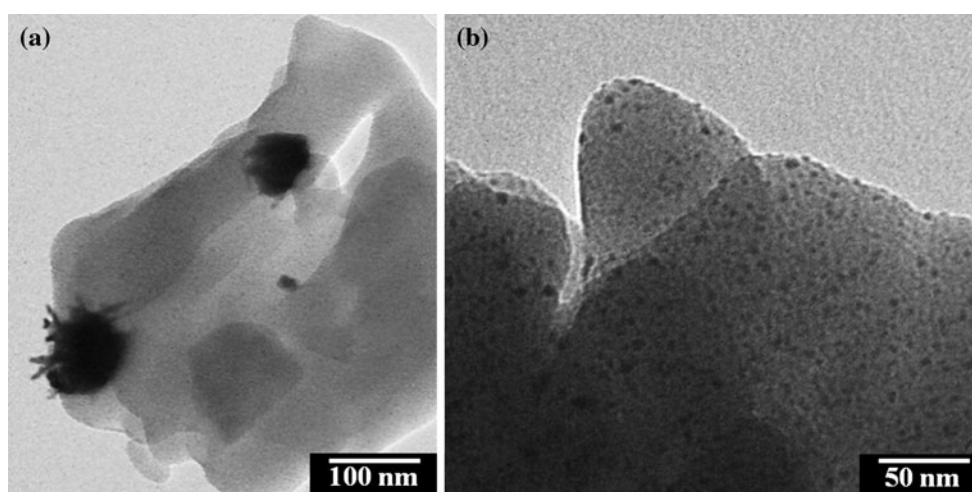

Fig. 2 Bright field TEM images of **a** platinum nanoparticles with nanowire-like structures on the surface and **b** platinum nanoclusters obtained after the reduction of the $PtCl_6^{-2}$/MOR and $Pt(NH_3)_4^{+2}$/MOR samples, respectively, with water saturated H_2 (method B)

surface of the zeolite while in the mesoporous silicas the nanowires were formed inside the pores. Overall, these results suggest that the water in the hydrogen promotes the diffusion of the Pt atoms from the $PtCl_6^{-2}$ to form elongated structures. This could be due to the affinity of this precursor with water that increases its mobility on the surface of the particle core.

The $Pt(NH_3)_4^{+2}$/MOR sample reduced with method B yielded dispersed nanoclusters with an average size of 2.2 nm (SD = 0.346 nm) as shown in Fig. 2b. These nanoclusters were smaller in size and more homogeneously distributed than those synthesized without the water saturation. The mechanism of this synthesis appears to be different than that using $PtCl_6^{-2}$ as a precursor and mesoporous silica as a template. In this article, the water molecules appear to either limit the diffusion of the Pt particles or increase the reaction rate of the reduction process. One possible explanation is that the water acts as a capping

agent for the nanoclusters either due to its preferred adsorption in the small cavities of the zeolite [34] or due to an hydration layer over the Pt.

Figure 3a shows the growth of nanostructures in the surface of the zeolite mordenite of the $PtCl_6^{-2}$/MOR reduced with formic acid. As in Fig. 2a these platinum structures appear to have nanowires growing from the surface of a spherical core. However, in contrast to Fig. 2a these cores are denser. The nanoparticles core is approximately 166 nm (SD = 50 nm) in diameter with very small (~4 nm diameter) nanowire-like structures on its surface.

This result can be contrasted to the results reported by Sun et al. [25] where using this precursor without a template formed single crystalline platinum nanoflowers with 150–400 nm diameter cores and 100–200 nm length nanowires. This suggests that the zeolite acts as a nucleation site promoting the formation of nanostructures with larger diameter cores and smaller nanowires. Meanwhile,

when comparing Fig. 3a with Fig. 2a and Fig. 1a, a general tendency can be observed toward the formation of anisotropic structures on the surface of spherical cores when using the $PtCl_6^{-2}$ in zeolite mordenite. This is a combination of the effects of the electrostatic repulsion of the precursor with the zeolite framework mentioned previously and the natural tendency of the $PtCl_6^{-2}$ to form anisotropic platinum nanostructures.

On the other hand, when the sample was impregnated with $Pt(NH_3)_4^{+2}$ and was reduced with formic acid, agglomerated platinum nanoclusters were formed inside zeolite mordenite. The average diameter of the nanoclusters was 5 nm (SD = 2 nm). The agglomeration of the platinum nanoclusters suggests a poor diffusion of the reducing agent into the zeolite at room temperature.

For comparison reasons, the same reduction method was done at 110° C. At this temperature, nanoparticles with an average diameter of 11 nm (SD = 5) were formed on the surface of the zeolite when using $PtCl_6^{-2}$, and 3.6 nm well-dispersed nanoclusters (SD = 0.8 nm) are formed inside the zeolite. The fact that more isotropic and smaller nanostructures are formed at this temperature agrees with the fact that at higher temperatures the reduction rate is higher than the diffusion rate leading to smaller nanoparticles. This is consistent with the fact that the reduction potential of any reducing agent increases with temperature.
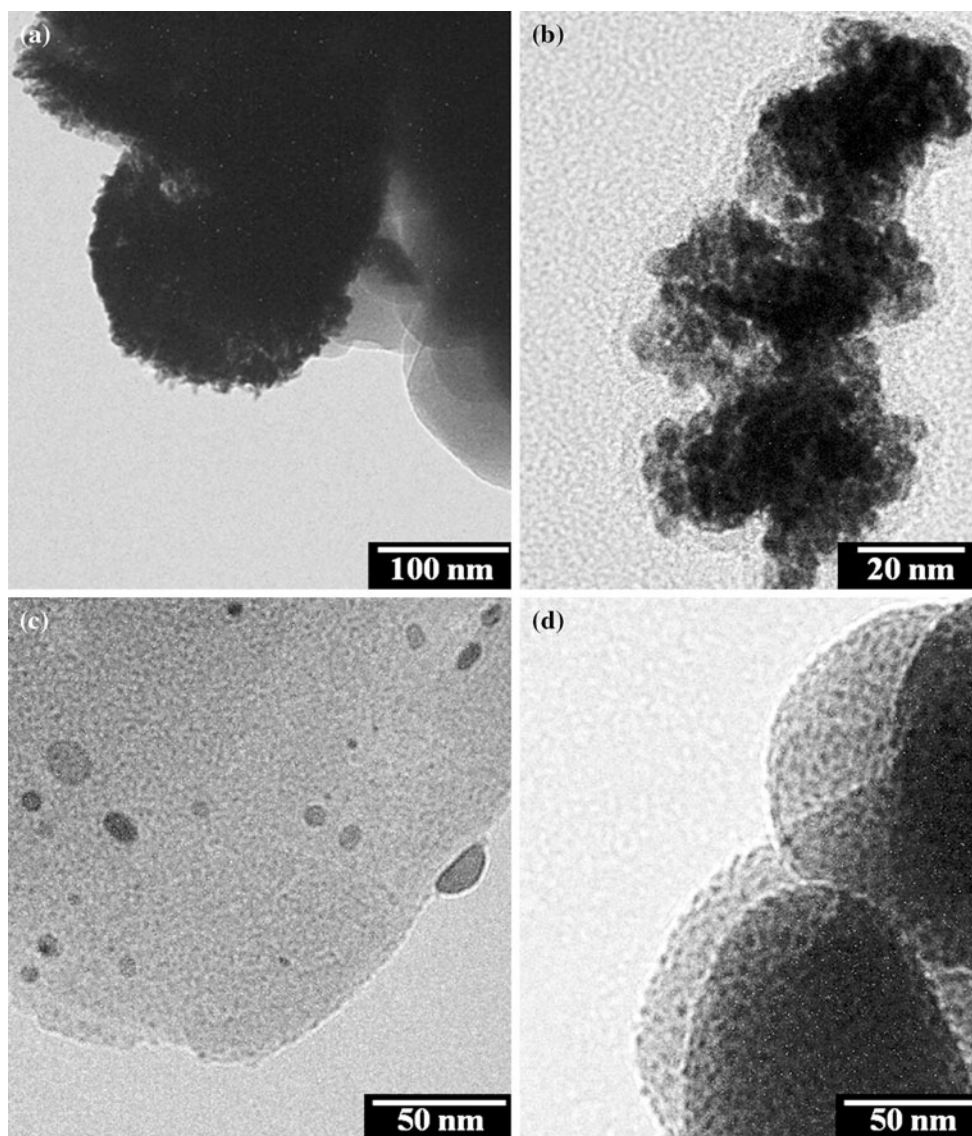

Fig. 3 Bright field TEM images of **a** platinum nanoparticles with nanowire-like structures on the surface and **b** agglomerated platinum nanoclusters, obtained after the reduction of the $PtCl_6^{-2}$/MOR and $Pt(NH_3)_4^{+2}$/MOR samples, respectively, using formic acid at room T (method C). **c** Platinum nanoparticles, and **d** dispersed platinum nanoclusters obtained after the reduction of the $PtCl_6^{-2}$/MOR and $Pt(NH_3)_4^{+2}$/MOR samples, at 110 °C (method C′)

This temperature is also slightly higher than the normal boiling temperature of the formic acid; so, its diffusion can be expected to be higher.

The reduction of a $PtCl_6^{-2}$/MOR sample with ethylene glycol at 110 °C leads to the formation of multipod platinum nanostructures with an average diameter of 24 nm (SD = 10 nm) as shown in Fig. 4a. Similar Pt multipod structures have been obtained in soft templates. However, in those studies [23, 24, 26] extraneous inorganic substances such as $NaNO_3$ and Ag(acac) were necessary to form the multipodic structures. This suggests that here the zeolite has an active role in affecting the anisotropy of the platinum structures.

The TEM image in Fig. 4b shows the formation of 5 nm nanoclusters (SD = 1.4 nm) in mordenite, after the reduction of $Pt(NH_3)_4^{2+}$/MOR with ethylene glycol. These results show a better nanoparticle distribution in comparison to the nanoclusters obtained with formic acid at room temperature and a comparable nanoparticle size and distribution at the same temperature (110 °C). This temperature was below the normal boiling point of ethylene glycol, which suggests that the temperature is a more influential factor than the diffusion of the reducing agent in the formation of nanoclusters when using $Pt(NH_3)_4^{2+}$ in mordenite.

When the same experiment was done at 200 °C, 14.5-nm diameter nanoparticles (SD = 6 nm) were formed on the surface of the zeolite when using $PtCl_6^{-2}$ as a precursor, and nanoclusters of 3 nm in diameter (SD = 1 nm) were formed inside the zeolite when $Pt(NH_3)_4^{+2}$ was used (Fig. 4 c and d, respectively). This temperature was above the normal boiling temperature of the ethylene glycol, and it is evident that the tendency toward the formation of anisotropic nanostructures when using $PtCl_6^{-2}$ is gone and
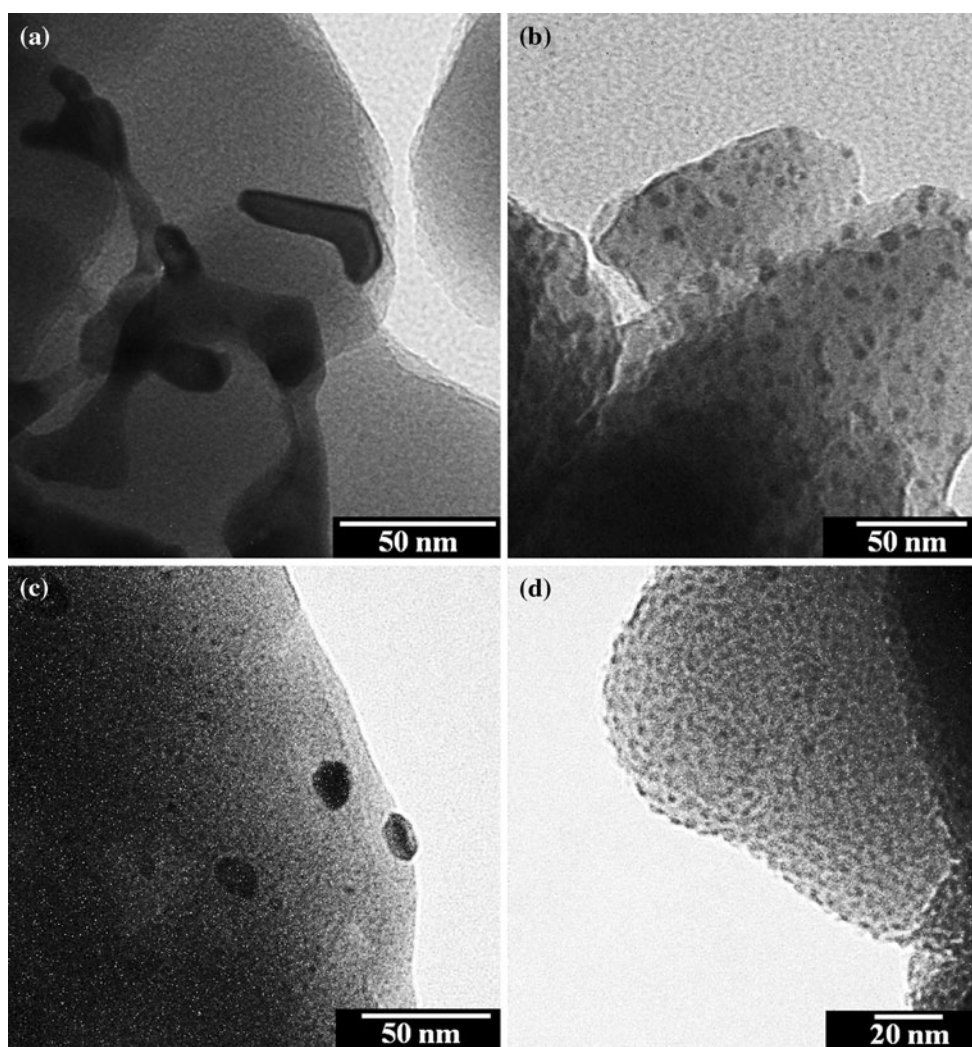

Fig. 4 Bright field TEM images of **a** platinum multipod and **b** platinum nanoclusters formed in $PtCl_6^{-2}$/MOR and $Pt(NH_3)_4^{+2}$/MOR, respectively, after the reduction with ethylene glycol at 110 °C (method D). **c** and **d** platinum nanoclusters obtained after the reduction of the $PtCl_6^{-2}$/MOR and $Pt(NH_3)_4^{+2}$/MOR samples with ethylene glycol at 200 °C (method D′)

Fig. 5 Bright field TEM images of nanoclusters formed in **a** $PtCl_6^{-2}$/MOR and **b** $Pt(NH_3)_4^{+2}$/MOR synthesized by UV-photoreduction (method E)

slightly smaller nanoclusters are formed with $Pt(NH_3)_4^{+2}$ at this temperature than at 110 °C. This suggests that the temperature and phase change affected the reduction of the $PtCl_6^{-2}$ more drastically than the $Pt(NH_3)_4^{+2}$.

Figure 5 shows the Pt nanoclusters formed for the samples reduced with method E on the surface of the sample reduced with UV. In the $PtCl_6^{-2}$/MOR sample (Fig. 5a), the Pt clusters were located on the surface of the zeolite with an average size of 5.3 nm (SD = 1.2 nm) while in the $Pt(NH_3)_4^{+2}$/MOR sample (Fig. 5b) they were well dispersed inside the zeolite pores with an average size of 1.5 nm (SD = 0.5 nm). This method yielded the most dispersed nanoclusters found in any of the reduction methods reported here. In fact, these results are comparable to results obtained through very strict traditional catalyst synthesis conditions. This is probably due to the fact that

there was no driving force for the diffusion of the Pt atoms as there was no reducing agent flowing through the pores of the zeolite. It is also possible that the methanol is acting as a capping agent much like the water in the water-saturated hydrogen reduction method.

Finally, the TEM images of the samples reduced with the reduction method F are shown in Fig. 6. Figure 6a corresponds to the $PtCl_6^{-2}$/MOR sample, and it shows the formation of large and small nanoparticles with irregular shapes formed on the surface of the zeolite. On the other hand, platinum nanowires with diameters in the range of 8–60 nm were formed inside of the zeolite mordenite when $Pt(NH_3)_4^{+2}$ was used as precursor as shown in Fig. 6b. The nanowires are evident as dark stripes around the external surface area of the zeolite. These results are qualitatively comparable to those found previously with $NaBH_4$ and
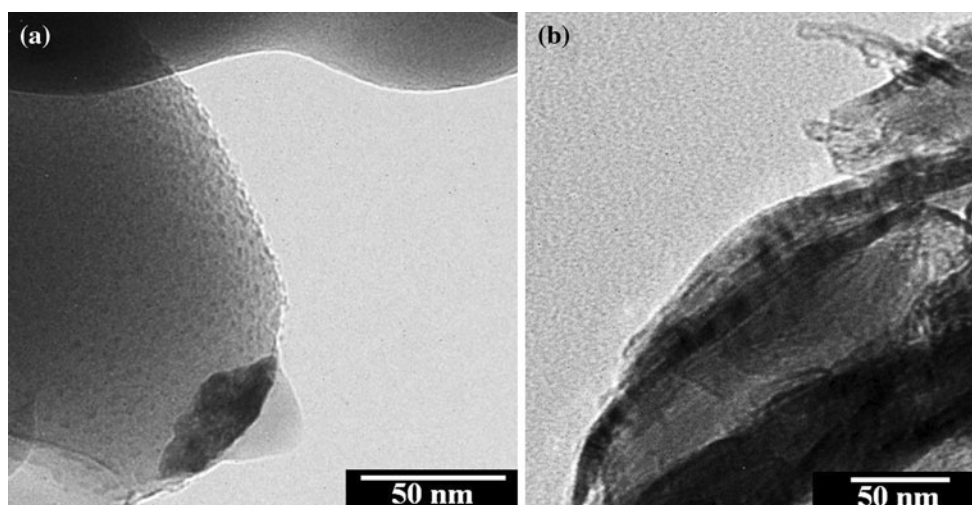

Fig. 6 Bright field TEM images of **a** platinum nanoclusters and **b** platinum nanowires formed in $PtCl_6^{-2}$/MOR and $Pt(NH_3)_4^{+2}$/MOR, respectively, after solid-state reduction with KBH_4 (method F)

demonstrate that KBH$_4$ is efficient for the formation of nanowires in porous materials when used in the solid state.

The formation of platinum nanowires using this method can be explained as an anodic electrochemical reaction that starts in the external surface of the zeolite. The slow evolution of this reaction promotes the migration and diffusion of positive platinum precursors from the internal zone of the zeolite toward the surface. Progressively, the positive platinum precursors that reach the platinum surface are reduced by the transfer of electrons promoting the formation of nanowires. In this process the KBH$_4$ is thought to have a very poor penetration into the pores of the zeolite such that it stays mainly on the surface.

Conclusions

There was an evident difficulty of the negatively charged precursor to diffuse inside the pores of the zeolite. The difficulty is associated with an electrostatic repulsion between the anodic precursor and the negative charges in the pore channels of the zeolite. As a consequence, all the nanostructures formed using this precursor grew unrestricted, forming large clusters on the surface of the zeolite. Nevertheless, there was a characteristic tendency for this precursor to form anisotropic nanostructures on the surface of the clusters as was found in the literature for other systems with the notable effect that the presence of the zeolite promoted the formation of a bigger core. Perhaps a way to form nanowires in zeolites with this precursor requires a modification of the zeolite's pore charge.

Comparing the results using the reducing agents at different states, it was evident that the anisotropy of the platinum nanostructures formed increased employing the sequence of Gas < Liquid < Solid. This can be explained by the slower diffusion of the reducing agent when going to denser phases. In general, it was observed that an anisotropic crystal growth was favorable when the synthesis is dominated by the diffusion of the Pt atoms when compared with the diffusion of the reducing agent and the reduction rate. This was achieved by using lower temperatures and denser reducing agents.

Zeolites have very small pores, which leads to a slow diffusion of molecules (both from the platinum precursor and the reducing agent). This causes syntheses of nanostructures to be controlled mostly by the reduction kinetics. Thus, in general, the formation of anisotropic structures inside of the zeolites is difficult when using gas and liquid reducing agents. On the other hand, and as was observed previously by our group, the use of a solid-state reducing agent yielded platinum nanowires inside of the zeolite.

These are very important reasons why the reduction methods studied, that have successfully yielded Pt nanowires in other systems, do not achieve similar results when using a zeolite as template, and a method such as the solid-state reduction method is necessary for the formation of such nanostructures in zeolites.

Finally, four reduction methods were found that could be further explored to synthesize supported platinum catalysts: through the use of water saturated hydrogen, the use of formic acid and ethylene glycol at temperatures higher than the normal boiling temperature and through UV reduction.

References

1. Xia Y, Yang P (2003) Adv Mater 15:351
2. Hrapovic S, Liu Y, Male KB, Luong JHT (2003) Anal Chem 76:1083
3. Chen H, Yuan R, Chai Y, Wang J, Li W (2010) Biotechnol Lett 32:1401
4. Yang H, Zhu Y (2007) Biosens Bioelectron 22:2989
5. Zhu N, Chang Z, He P, Fang Y (2005) Anal Chim Acta 545:21
6. Yang M, Yang Y, Liu Y, Shen G, Yu R (2006) Biosens Bioelectron 21:1125
7. Yang M, Qu F, Lu Y, He Y, Shen G, Yu R (2006) Biomaterials 27:5944
8. Fengli Q, Minghui Y, Guoli S, Ruqin Y (2007) Biosens Bioelectron 22:1749
9. Sasaki M, Osada M, Sugimoto N, Inagaki S, Fukushima Y, Fukuoka A, Ichikawa M (1998) Microporous Mesoporous Mater 21:597
10. Adhyapak PV, Karandikar P, Vijayamohanan K, Athawale AA, Chandwadkar AJ (2004) Mater Lett 58:1168
11. Tiemann M (2007) Chem Mater 20:961
12. Sakamoto Y, Fukuoka A, Higuchi T, Shimomura N, Inagaki S, Ichikawa M (2003) J Phys Chem B 108:853
13. Chen A, Holt-Hindle P (2010) Chem Rev 110:3767
14. Song Y, Garcia RM, Dorin RM, Wang H, Qiu Y, Coker EN, Steen WA, Miller JE, Shelnut JA (2007) Nano Lett 7:3650
15. Webb P, Orr C, Camp R, Olivier J, Yunes Y (1997) Analytical methods in fine particle technology. Micromeritics Instrument Corporation, Norcross, GA
16. Napolskii KS, Barczuk PJ, Vassiliev SY, Veresov AG, Tsirlina GA, Kulesza PJ (2007) Electrochim Acta 52:7910
17. Yang C-M, Sheu H-S, Chao K-J (2002) Adv Funct Mater 12:143
18. Araki H, Fukuoka A, Sakamoto Y, Inagaki S, Sugimoto N, Fukushima Y, Ichikawa M (2003) J Mol Catal A: Chem 199:95
19. Fukuoka A, Sakamoto Y, Higuchi T, Shimomura N, Ichikawa M (2006) J Porous Mater 13:231
20. Fukuoka A, Higashimoto N, Sakamoto Y, Inagaki S, Fukushima Y, Ichikawa M (2002) Top Catal 18:73
21. Fukuoka A, Higuchi T, Ohtake T, Oshio T, Kimura J-i, Sakamoto Y, Shimomura N, Inagaki S, Ichikawa M (2006) Chem Mater 18:337
22. Fukuoka A, Higashimoto N, Sakamoto Y, Sasaki M, Sugimoto N, Inagaki S, Fukushima Y, Ichikawa M (2001) Catal Today 66:23

23. Chen J, Herricks T, Geissler M, Xia Y (2004) J Am Chem Soc 126:10854
24. Herricks T, Chen J, Xia Y (2004) Nano Lett 4:2367
25. Sun S, Yang D, Villers D, Zhang G, Sacher E, Dodelet J (2008) Adv Mater 20:571
26. Teng X, Yang H (2005) Nano Lett 5:885
27. Chakarova K, Hadjiivanov K, Atanasova G, Tenchev K (2007) J Mol Catal A: Chem 264:270
28. Yang Y-X, Bourgeois L, Zhao C, Zhao D, Chaffee A, Webley PA (2009) Microporous Mesoporous Mater 119:39
29. Quiñones L, Grazul J, Martínez-Iñesta MM (2009) Mater Lett 63:2684
30. Sakamoto Y, Fukuoka A, Higuchi T, Shimomura N, Inagaki S, Ichikawa M (2003) J Phys Chem B 108:853
31. Kubanek P, Schmidt HW, Spliethoff B, Schüth F (2005) Microporous Mesoporous Mater 77:89
32. Ismagilov ZR, Yashnik SA, Startsev AN, Boronin AI, Stadnichenko AI, Kriventsov VV, Kasztelan S, Guillaume D, Makkee M, Moulijn JA (2009) Catal Today 144:235
33. Rivallan M, Seguin E, Thomas S, Lepage M, Takagi N, Hirata H, Thibault-Starzyk F (2010) Angew Chem Int Ed 49:785
34. Rees L, Shen D (2001) In: Jansen J (ed) Studies in surface science and catalysis, vol 137. Elsevier Science, Amsterdam